J Neurophysiol 116: 1286–1294, 2016.
First published June 22, 2016; doi:10.1152/jn.00197.2016.

CALL FOR PAPERS | *Methods to Understand Brain Connections and Neural Function*

Optogenetic manipulation of neural circuits in awake marmosets

Matthew MacDougall,[1,2] Samuel U. Nummela,[2] Shanna Coop,[2] Anita Disney,[5] Jude F. Mitchell,[4,6] and Cory T. Miller[2,3,4]

[1]*Department of Neurosurgery, University of California, San Diego, La Jolla, California;* [2]*Cortical Systems and Behavior Laboratory, University of California, San Diego, La Jolla, California;* [3]*Neurosciences Graduate Program, University of California, San Diego, La Jolla, California;* [4]*Kavli Institute for Brain & Mind, University of California, San Diego, La Jolla, California;* [5]*Department of Psychology, Vanderbilt University, Nashville, Tennessee; and* [6]*Department of Brain and Cognitive Sciences, University of Rochester, Rochester, New York*

Submitted 7 March 2016; accepted in final form 21 June 2016

MacDougall M, Nummela SU, Coop S, Disney A, Mitchell JF, Miller CT. Optogenetic manipulation of neural circuits in awake marmosets. *J Neurophysiol* 116: 1286–1294, 2016. First published June 22, 2016; doi:10.1152/jn.00197.2016.—Optogenetics has revolutionized the study of functional neuronal circuitry (Boyden ES, Zhang F, Bamberg E, Nagel G, Deisseroth K. *Nat Neurosci* 8: 1263–1268, 2005; Deisseroth K. *Nat Methods* 8: 26–29, 2011). Although these techniques have been most successfully implemented in rodent models, they have the potential to be similarly impactful in studies of nonhuman primate brains. Common marmosets (*Callithrix jacchus*) have recently emerged as a candidate primate model for gene editing, providing a potentially powerful model for studies of neural circuitry and disease in primates. The application of viral transduction methods in marmosets for identifying and manipulating neuronal circuitry is a crucial step in developing this species for neuroscience research. In the present study we developed a novel, chronic method to successfully induce rapid photostimulation in individual cortical neurons transduced by adeno-associated virus to express channelrhodopsin (ChR2) in awake marmosets. We found that large proportions of neurons could be effectively photoactivated following viral transduction and that this procedure could be repeated for several months. These data suggest that techniques for viral transduction and optical manipulation of neuronal populations are suitable for marmosets and can be combined with existing behavioral preparations in the species to elucidate the functional neural circuitry underlying perceptual and cognitive processes.

ChR2; cortex; marmoset; neurophysiology; optogenetics

NEW & NOTEWORTHY

Marmosets have emerged as a valuable model for applying modern molecular techniques to the study of the primate brain. We developed a novel, chronic preparation for optogenetic photostimulation of cortical neurons in awake marmosets. This approach is well suited for use in studies aimed at investigating functional neural circuitry in behaving marmosets.

THE ARCHITECTURE OF HUMAN and nonhuman primate neocortex has been relatively conserved across the evolution of our Order (Chaplin et al. 2013; Kaas 2006). These shared neural processes likely underlie the many aspects of social behavior and cognition characteristic of all primate species (Seyfarth and Cheney 2014). Rhesus monkeys (*Macaca mulatta*) have been the dominant model for studies of neural function in primates for many decades. Not surprisingly, the first applications of optogenetic methods to manipulate neural circuits and behavior in primates have been performed in rhesus monkeys. Systematic investigation of viral transduction and the development of methods for photostimulation in awake rhesus monkeys (Diester et al. 2011; Han et al. 2009) laid the foundation for subsequent studies that applied these methods to studies of behavior and perception (Afraz et al. 2015; Cavanaugh et al. 2012; Geritis et al. 2012; Jazayeri et al. 2012; Ohayon et al. 2013). These experiments demonstrate the potential for manipulating neural circuits in primate brains with optogenetic techniques. However, the magnitude of the behavioral effects observed in these studies has been notably less robust than in many of the comparable studies in rodents (Geritis and Vanduffel 2013). Although several factors likely contribute to this trend, it does suggest that additional work is needed to optimize these methods for primates.

The marmoset has emerged as a potentially important neuroscientific model, in part because of its suitability for gene-editing techniques (Belmonte et al. 2015; Sasaki et al. 2009). This small-bodied New World monkey has several advantages to further develop and optimize many of the cutting-edge molecular and imaging techniques employed in neuroscience for studies of nonhuman primate neural circuitry and behavior, including optogenetics. First, the marmoset brain is almost entirely lissencephalic (smooth). This allows direct access to most cortical areas directly beneath the skull and may facilitate mapping functional neuronal circuits using adeno-associated virus (AAV) constructs (Oh et al. 2014). Second, despite the smaller size, the core architecture of primate neocortex has been conserved in this species, making direct comparisons to other primates, including humans, feasible (Chaplin et al. 2013; Mitchell and Leopold 2015). Third, their relatively high fecundity for a primate (4–6 babies a year) and small body size allow for a single laboratory to feasibly house a large colony with an adequate population size to systematically test and optimize

Address for reprint requests and other correspondence: C. T. Miller, Univ. of California, San Diego, 9500 Gilman Drive #0109, La Jolla, CA 92093 (e-mail: corymiller@ucsd.edu).

these techniques. Fourth, marmosets engage in both natural (Chow et al. 2015; Miller and Thomas 2012) and conditioned (Mitchell et al. 2014; Osmanski et al. 2013; Song et al. 2016) behavioral tasks under laboratory conditions that are amenable to modern molecular techniques. Thus far, few studies have determined whether these potential benefits translate into new insights into primate brain function.

In this study we sought to test the suitability of marmosets for manipulating neural populations with optical stimulation techniques in awake subjects. Previous work has shown that certain combinations of AAV serotype and promoter in viral constructs express robustly in the marmoset brains (Masamizu et al. 2010, 2011; Watakabe et al. 2015). No studies have yet examined whether particular constructs are ideal for achieving physiological changes in membrane potential following transduction of channelrhodopsin (ChR2) for the marmoset. To this end, we developed a chronic preparation for delivering light stimuli that allows for repeated, aseptic, physical access to the marmoset brain for electrodes. Using this preparation, we demonstrate precise optogenetic manipulation of neocortical neurons expressing channel-rhodopsin in awake marmosets. These findings form the foundation for subsequent manipulation of neural circuits during behavioral tasks.

MATERIALS AND METHODS

Subjects. Two adult female marmosets (*Callithrix jacchus*), *subjects J* and *Y*, were used for neurophysiological recordings during optical stimulation. An additional two adult marmosets, one male and one female, were used to histologically examine viral transduction in the species. Subjects were group housed in the Cortical Systems and Behavioral Laboratory at University of California, San Diego (UCSD). All experimental protocols were approved by the UCSD Institutional Animal Care and Use Committee and were conducted in compliance with National Institutes of Health guidelines for animal research.

Surgical procedure: optogenetics. Under general anesthesia, a parasagittal strip of scalp ~1 cm in width and 2 cm anterior-posterior was removed beginning from just behind the supraorbital fat pad. The skull periosteum was bluntly dissected laterally, and the superior 2–4 mm of temporalis muscle bilaterally were elevated, cauterized, and resected. The exposed skull was rinsed, and 1-mm craniotomies were drilled in several locations throughout the exposed skull. Surgical screws (1.5 mm; Synthes) were inserted into the craniotomies to act as anchors for the acrylic head cap. A central steel head post was held in place over the bregma, and successive layers of dental acrylic were applied and allowed to cure over the head post and screws. The monkey was given a minimum of 4 wk to recover.

Once subjects recovered from the initial surgery, we performed a second procedure for the chronic optogenetic preparation. Under ketamine-lorazepam sedation and with the animal restrained using the head post, a Dremel was used to drill a 5- to 8-mm-diameter hole in the acrylic head cap to expose skull. A drill was mounted on a micromanipulator, and a 2- to 3-mm-diameter craniotomy was made. An automated injector was then mounted on the micromanipulator, and a 5-μl Hamilton syringe with a pulled glass tip was advanced until it pierced dura. Injections of 2.5 μl each were made at two depths, 1.0 and 1.5 mm, separated by a 5-min pause. The needle remained in place for 5 min following injection before removal. A single viral vector construct (AAV5.hSyn.ChR2.eYFP) was injected in each craniotomy.

A schematic of the chronic optical stimulation preparation is shown in Fig. 1. After the viral injection, a 200-μm, 0.22-NA, 1-cm fiber-optic cannula (ThorLabs) was placed just through the dura above the virally infected area. The fiber-optic cannula was advanced through a small incision in the dura and embedded in the wall of the chamber with dental acrylic. This served to stabilize the cannula and limit movement. A 5-mm ThorLabs coupler, included with the cannula, was used to connect the cannula to a longer fiber-optic cable to deliver light stimuli. A surgical steel ground wire was placed under the edge of the craniotomy and bent such that it protruded out of the chamber before being embedded into the chamber wall with dental acrylic. Finally, silastic gel (Kwik-Sil; World Precision Instruments) was injected over the dura and allowed to cure, creating a transparent, penetrable seal ~2 mm in thickness. Once dried, either the cured edge of the silastic was glued to the skull or acrylic was placed just over its border to ensure a tight seal and hold the silastic in place. When not in use, the chamber and surface of the silastic were cleaned with sterile saline, filled with bacitracin ointment, and covered with a rubber cap. The silastic remained in place for the duration of the study. We have observed both in these experiments and in others (Miller et al. 2015) that silastic, when applied correctly, limits the growth of granulation tissue on the dura over long periods (6–12 mo). Because of this characteristic, the silastic was not removed, nor was dura cleaned, during these experiments. The craniotomy in *subject J* was performed over temporal cortex, whereas the craniotomy in *subject Y* was performed over frontal cortex.

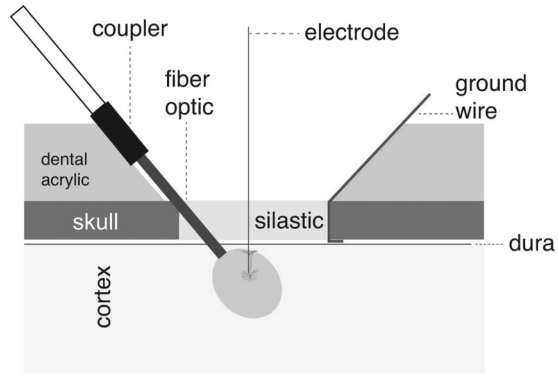

Fig. 1. Schematic of chronic preparation for optogenetic photostimulation in marmosets. Drawing shows the design of the preparation used for these experiments. After a craniotomy, a fiber-optic cannula is inserted below dura. During experiments, a plastic coupler connects the cannula with a longer fiber-optic cable to deliver light stimuli. A ground wire inserted between the skull and dura is shown. Silastic is used to fill the craniotomy. Dental acrylic is used to cement the fiber-optic cannula and ground wire in place. Electrodes can pass freely through the silastic without damage to record neural responses during delivery of light stimulus.

Surgical procedure: viral injections for histological analysis. With the use of general anesthesia and stereotaxic head fixation, a 2-cm sagittal incision was made in the scalp, which was retracted laterally. A drill was mounted on a micromanipulator and 0.5-mm craniotomies were made 3–4 mm lateral to the sagittal midline. Injections were performed following the procedure outlined above. At the conclusion of the surgery, the scalp was sutured and the monkey recovered. Virus was allowed to express for 4 wk prior to death for histologic examination. We chose injection sites primarily with regard for convenient and safe access to the brain given the limitations of each particular marmoset's head cap such that there was no standard cortical location for the injections.

Viruses. Stocks of adeno-associated virus (AAV) constructs were obtained from the University of Pennsylvania Vector Core. Stocks of virus were maintained at −80°C until they were thawed just before injection. The following constructs were used: AAV5.hSyn.ChR2(H134R).eYFP.WPRE.hGH (Addgene26973; titer: 1.42e13 GC/ml) and AAV9.hSyn.ChR2(H134R).eYFP.WPRE.hGH (Addgene26973P; titer: 2.75e13 GC/ml).

Neurophysiology and optical stimulation. With the animal awake and restrained by head fixation, a single 2.5- to 5-MΩ tungsten electrode (FHC) was mounted on a micromanipulator and advanced

through the silastic plug and dura, and then into cortex. The electrode was connected to an RA4PA Medusa PreAmp and an RZ6 (TDT) recording system. The digital output ports of the RZ6 were used to control a 100-mW, 473-nm diode-pumped solid-state (DPSS) fiber-coupled laser (LaserGlow) using TTL or analog signals. In preliminary tests, we also used a light-emitting diode (LED) module (25 mW, 465 nm; PlexBright) but found the lower power light did not produce reliable activation. The laser was connected to the implanted fiber cannula via a 200-μm multimode 0.22-NA fiber of 1 m in length. Single-unit responses were identified using custom MATLAB software (briefly, bandpass filtered from 300 Hz to 8 kHz, -3 dB, 6th-order Butterworth filter, thresholded to identify spikes, waveforms aligned at the trough, and manually clustered using 1st and 2nd principle components of waveforms). Photostimulation was delivered using several patterns of laser activation, including continuous pulses ranging from 75 to 500 ms, trains of 20-ms pulses at 50 Hz for 400 ms, or trains of 75-ms pulses at 13.3 Hz for 750 ms. Units were included in further analysis if $<$1% of responses occurred within 1 ms and firing rate changed between the 100 ms preceding photostimulation and the duration of photostimulation according to a signed-rank test ($P < 0.05$). Increases in neuron responses were classified as excitation and decreases as suppression. Time to excitation and suppression was calculated by comparing firing rate from laser pulse onset in 5-ms bins and finding the first bin that clearly differed from the 100 ms preceding photostimulation (signed-rank test, $P < 0.0001$).

Histology. At the conclusion of each experiment, the animals were killed by an intramuscular injection of ketamine-lorazepam, followed by an intraperitoneal injection of pentobarbital sodium. Intracardiac perfusion was performed using saline containing heparin, followed by 4% paraformaldehyde. The brain was then removed from the skull and placed in paraformaldehyde overnight, followed by 3 increasing concentrations of sucrose: 10%, 20%, and 30%. With the use of a cryotome, 40-μm coronal slices were cut, and slices were preincubated with 10% normal goat serum (Life Technologies) at 4°C for 1 h. Floating sections were incubated with primary antibodies in PBS-1% Triton X-100 at 4°C overnight.

After PBS rinses, the sections were incubated with secondary antibodies in PBS at 4°C for 5 h. Secondary antibodies were Alexa Fluor goat anti-mouse 594 or 488 IgG (1:500) or Alexa Fluor goat anti-rabbit 594 or 488 IgG (1:500; Life Technologies). Secondary antibody color was chosen in each case to not conflict with the virally transduced fluorescent tag. Primary antibodies against the following marker proteins were used, listed with their respective concentrations, such as NeuN (mouse, 1:500; Millipore).

The sections were mounted on gelatinized slides, dried at room temperature overnight, and dehydrated in 50, 70, 95, and 100% EtOH for 20 s. Sections were then incubated 2 times for 5 min in xylene and coverslipped with DPX. High-magnification images were collected using a Zeiss LSM710 laser scanning confocal microscope. The 488-nm laser line was used for fluorophore excitation at a power of 2.0% with a pinhole set to 33 μm. Cell bodies at the injection site and the corresponding contralateral cortical location were imaged using first the $\times$20 and then the $\times$63 (oil immersion) objective.

RESULTS

We developed a chronic preparation for optogenetic photostimulation of virally transduced neurons in awake marmosets. Using this preparation, we were able to record isolated single units from the same population of neurons over the course of several weeks and months following an injection of the viral construct AAV5.hSyn.ChR2.eYFP (Fig. 2). Individual neurons exhibited two types of responses during delivery of light stimuli: increases in firing rate, referred to as excitation, and decreases in firing rate, referred to as suppression. Single-unit responses were classified as excitation if firing rate significantly increased during photostimulation compared with the previous 100 ms, and as suppression if firing rate significantly decreased (signed-rank test, $P < 0.05$). Figure 2 shows plots of exemplar neurons exhibiting either excitation (Fig. 2, *left*) or suppression (Fig. 2, *right*) in response to light stimuli. A raw single-trial recording of neural responses during photostimulation in the *top* row demonstrates excitation (Fig. 2*A*) and suppression (Fig. 2B). Raster plots and peristimulus time histograms of neuronal firing for trains of either 20- or 75-ms light pulses characterize the responses of an individual excited neuron (Fig. 2, *C* and *E*) and suppressed neuron (Fig. 2, *D* and *F*). In both cases, neurons exhibited rapid changes in neural activity closely coupled to the onset and offset of the light stimulus.

A total of 66 isolated single cortical neurons were recorded from 2 awake marmosets, *subjects J* and *Y*. Fifty of these single units exhibited significant changes in firing rate during presentation of the light stimulus compared with the 100 ms preceding photostimulation (signed-rank test, $P < 0.05$), whereas 16 were not affected by the same stimulus (Fig. 3). A total of 24 neurons from this population exhibited significant excitation and 26 exhibited significant suppression during delivery of light stimuli (Fig. 3). We found that the minimum power necessary to drive neurons in this preparation ranged between 40 and 60 mW. The first neuron exhibiting photoactivation in each subject was not evident for several weeks following the injection of the viral construct. For *subject J*, the first photoactivated unit was recorded 48 days after the viral injection, whereas the first photoactivated neuron in *subject Y* did not occur for 50 days. Unit recordings were performed at least once per week until significant effects were observed, and significant effects were consistently observed for subsequent unit recordings.

To summarize the time course of excitation and suppression, Fig. 4*A* plots the overall change in firing rate against the time to the initial change in firing rate, at a resolution of 5 ms (see METHODS), and Fig. 4*B* shows the time to return to baseline activity following photostimulation offset. Figure 4*C* shows histograms of time to initial photostimulation. Whereas both excitation and inhibition tended to occur quickly, within 15 ms of pulse onset, excitation occurred significantly more quickly (rank-sum test, $P < 0.01$), rarely taking more than 10 ms. Figure 4*D* shows histograms of time from laser offset to return of baseline activity. Importantly, neurons showing suppression typically took much longer to return to baseline than excitation (rank-sum test, $P < 0.001$). Figure 4*E* provides a summary of the changes in activity by plotting firing rate during photostimulation against baseline firing rate during the 100 ms preceding photostimulation. The total change in firing rate was lower for suppression than for excitation, but this may be due to low baseline firing rates. When suppression occurred it often completely suppressed activity for the duration of photostimulation.

One of the key aims of this study was to develop a stable preparation for delivering light and inducing optical stimulation effects over long periods of time. This was because of the explicit goal of developing a preparation that could be implemented in future studies involving behaving animals. Although most recordings occurred in the first two mo following the initial viral injection, we also performed 3 recording sessions 9

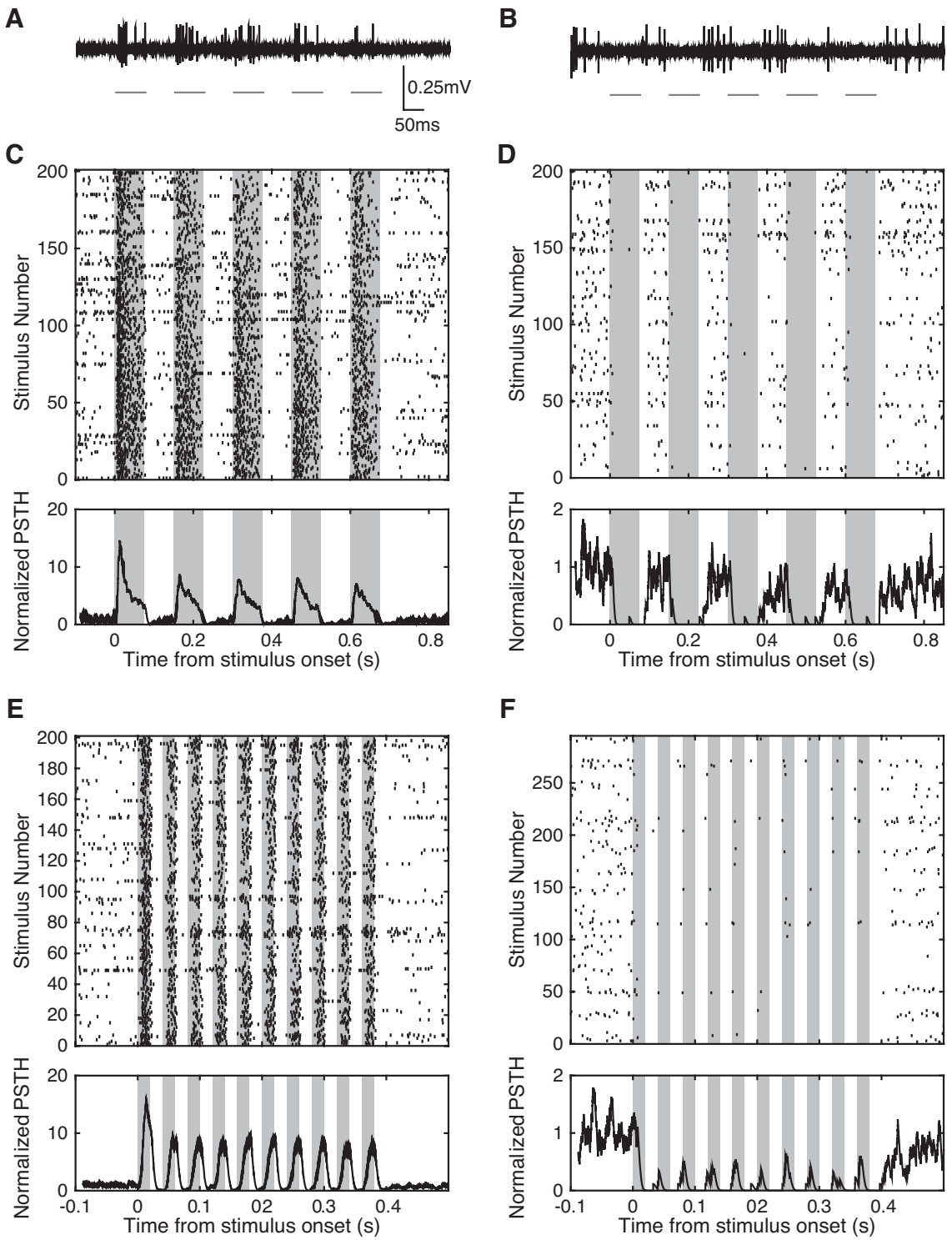

Fig. 2. Excitation and suppression of single-unit activity in response to photostimulation. *A* and *B*: sample wave forms exhibiting excitation (*A*) and suppression (*B*) in response to a 13.3-Hz train of 75-ms laser pulses (*B* has the same scale as *A*). *C* and *D*: sample single-unit raster plots and peristimulus time histograms (PSTHs) of excitation (*C*) and suppression (*D*) in response to photostimulation at 13.3 Hz. *E* and *F*: sample single-unit raster plots and PSTHs of excitation (*E*) and suppression (*F*) in response to 50-Hz trains of 20-ms laser pulses. PSTHs were created by spike convolution with a half-Gaussian, $\sigma = 4$ ms, and were normalized to the average value 100 ms before photostimulation. *A*, *C*, and *E* plot the responses of a single neuron, whereas *B*, *D*, and *F* plot the responses of a different individual neuron.

mo after the virus injection in *subject J* to test the stability of the preparation. We found that we were still able to consistently elicit photostimulation effects in isolated single neurons (Fig. 4*E*). It is noteworthy that all of the neurons ($n = 6$) recorded after 9 mo were suppressed. This differed from the more equal distribution in previous recording sessions within the first 3–4 mo following the viral injection. Given that the overall distribution of interneurons in marmoset cortex paral-

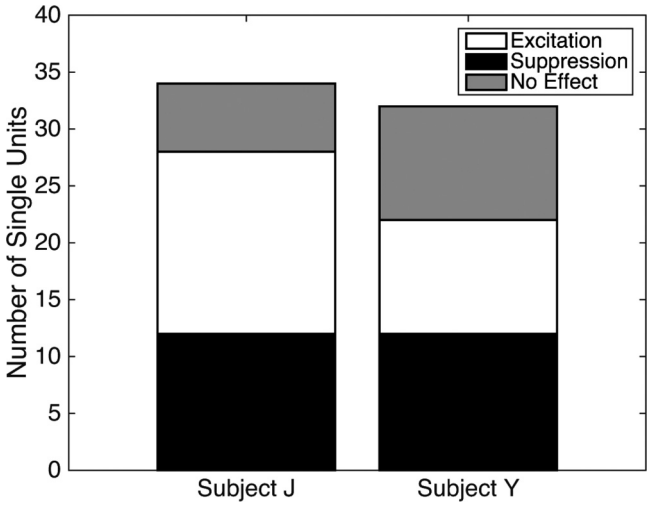

Fig. 3. Neural responses to light stimuli. Data are the number of single units showing significant excitation, significant suppression, or no effect for each subject. In each subject, more than a third of single units sampled within 1.5 mm of the injection site showed a response to photostimulation, with about half of the units showing excitation and half showing suppression of unit firing.

lels that of other primates (Goodchild and Martin 1998; Spatz et al. 1994), the observed pattern cannot be attributed to intrinsic differences in marmoset cortex. Instead, the prevalence of inhibitory responses during photoactivation, particularly after 9 mo, may be the result of preferential viral infection and deterioration of different cell types in the marmoset brain. Because of the small sample size, we cannot distinguish between these possibilities and the results should be considered preliminary. Furthermore, a Fishers Exact test comparing these 6 neurons with the first 6 recorded did not reach significance ($P = 0.07$). This is, however, an issue that we plan to pursue more systematically in future experiments.

Consistent with previous studies in marmosets (Masamizu et al. 2010, 2011; Watakabe et al. 2015), AAV viral constructs express robustly in cortex in these experiments. Figure 5 shows representative tissue samples from marmoset cortex following viral injections using AAV serotypes 5 and 9. As is evident, viral expression with both serotypes exhibited grossly similar patterns of expression. Laminar differences were evident, as expression was stronger in superficial and deep layers than in layer 4.

Viral expression for constructs comprising AAV9 serotype exhibited long-range anterograde and retrograde expression. Figure 6*A* shows transduction following injection of a single AAV9.hSyn.ChR2.eYFP construct in somatosensory cortex. The sections used for the images in Fig. 6 were not from subjects used in the photostimulation experiments. Expression was evident 3–6 mm laterally from the site of injection and across all layers of cortex as well as in projections from the injection site. Fluorescence was evident in discrete sites distant from the site of injection, including the corresponding contralateral hemisphere. Transduction to the contralateral hemisphere followed a distinct tract including corpus callosum fibers, ipsilateral caudate, thalamus, internal capsule, and cerebral peduncle. Expression in both the ipsilateral (Fig. 6*B*) and contralateral (Fig. 6*C*) hemispheres exhibited characteristic

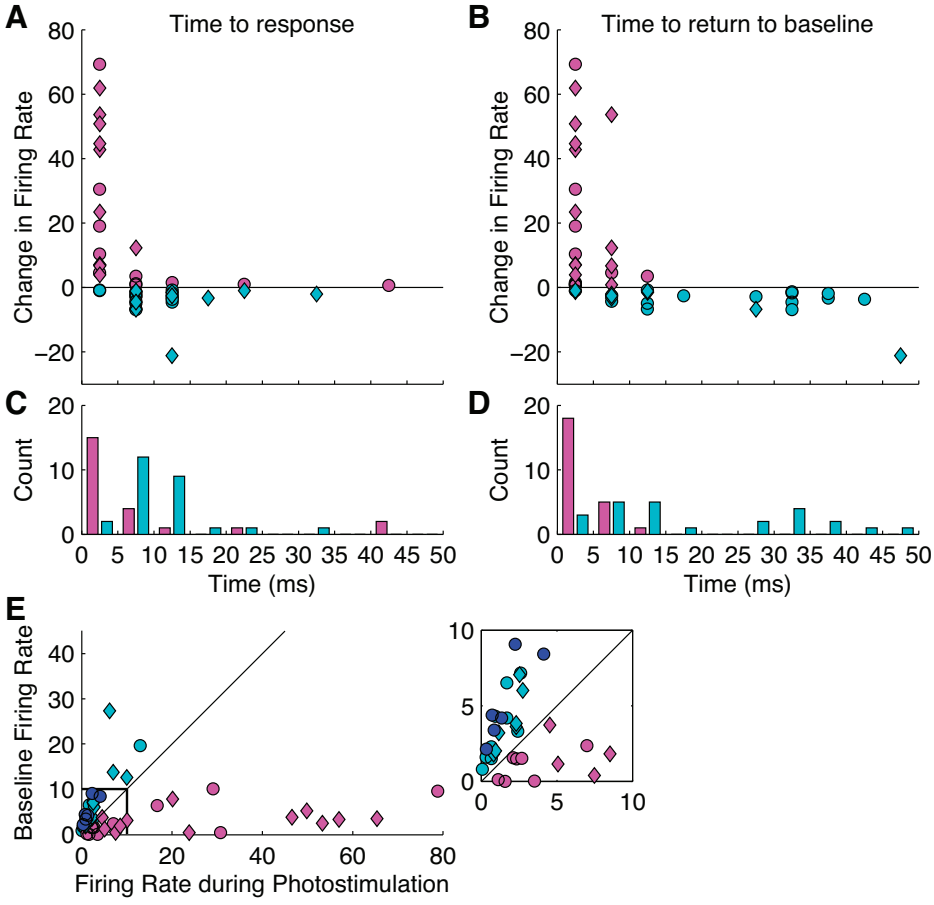

Fig. 4. Summary of the magnitude and latency of photostimulation. *A*: change in firing rate caused by photostimulation plotted against the time to the initial effect of photostimulation. We plot the "time to response" as the latency from the onset of the light stimulus until a neuron's firing rate is significantly above the prestimulus baseline period. *B*: change in firing rate caused by photostimulation plotted against the time from laser offset to a return to baseline activity. We plot latency from the offset of the light stimulus until firing rate returns to prestimulus baseline level. *C*: histograms of the latency to excitation and suppression from onset of photostimulation. *D*: histograms of the latency to baseline activity from photostimulation offset for neurons showing excitation and suppression. *E*: baseline firing rates plotted against firing rates during photostimulation for all units. Single units recorded 9 or more months from virus injection are represented in dark blue, and all exhibited suppression. An expanded view of the area outlined in black is shown in the *inset*. For *A–E*, circles correspond to *subject J* and diamonds to *subject Y*; magenta indicates excited neurons, and cyan indicates suppressed neurons. Dark blue circles in *E* indicate neurons recorded 9 mo after virus injection in *subject J*.

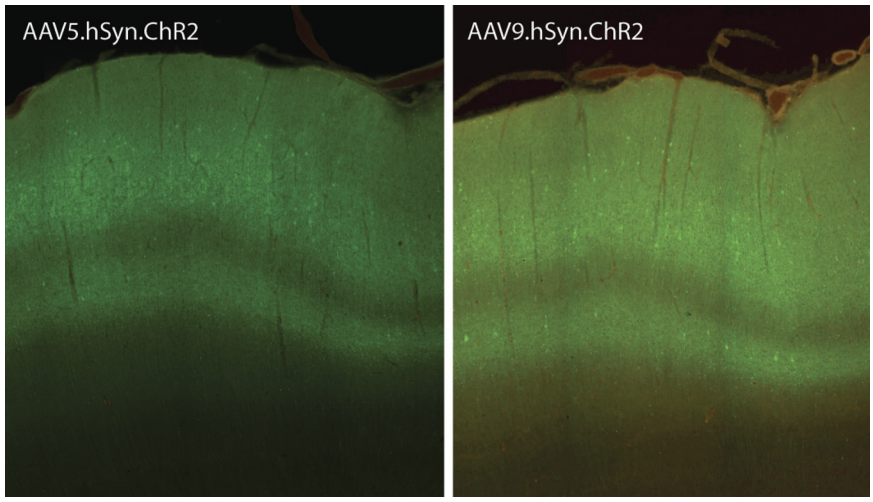

Fig. 5. Comparison of AAV serotype expression. Example tissue sections show viral transduction for AAV constructs for AAV5 (*left*) and AAV9 serotypes (*right*). Overall, we observed relatively similar patterns of expression with both of these serotypes, including a characteristic laminar pattern.

laminar patterns of expression, although the expression was stronger at the injection site. Although evident, the number of neurons in both the ipsi- and contralateral hemispheres expressing enhanced yellow fluorescent protein (eYFP) was notably sparse (Fig. 6, *D* and *E*). In fact, we found five or fewer clearly labeled cell bodies in both the ipsi- and contralateral hemispheres. As a result, further quantification was not possible. Viral transduction was also most evident in cell processes in the labeled subcortical structures, such as thalamus (Fig. 6*F*) and putamen (Fig. 6*G*). Although it is clear that the virus was able to infect axons at the injection site and travel retrograde to cause expression in contralateral cell bodies (Fig. 6, *D* and *E*), these results should be considered preliminary.

Previous work has shown that AAV can be used to label long-range projections in mice (Oh et al. 2014) and rhesus monkeys (Masamizu et al. 2011; Salegio et al. 2014; San Sebastian et al. 2013), but there is much variability in anterograde or retrograde transport depending on the serotype (Salegio et al. 2014; San Sebastian et al. 2013). Although we found preliminary evidence that at least AAV9 constructs led to expression in cell bodies in the contralateral hemisphere, we were unable to confirm that viral constructs comprising the AAV5 serotype showed a similar pattern of long-range projections. The prospect of labeling long-range projection neurons in marmoset cortex with AAV viral constructs is highly valuable as a tool for studies of neural circuitry, but a more systematic study is required to confirm our observations and quantify the patterns of viral expression more fully.

DISCUSSION

Marmosets have emerged as a key model for studying primate neuronal function (Miller et al. 2016), in part driven by the opportunity to apply modern gene-editing techniques in a primate brain to investigate numerous questions pertaining to functional neural circuitry (Belmonte et al. 2015; Sasaki et al. 2009). In this study we tested the suitability of this nonhuman primate species for manipulating neural circuits using optical stimulation techniques. To manipulate neural circuits with optical stimulation, we developed a preparation with a chronically implanted fiber optic to deliver light stimuli to a population of neurons following viral injections. We used AAVs to deliver channelrhodopsin and were able to induce rapid changes in the activity in single neurons expressing channelrhodopsin (ChR2) in awake marmosets during stimulation with this preparation. Our results suggest that the application of these techniques in marmosets may be a valuable tool for elucidating the functional neural circuitry in the primate brain.

Channelrhodopsin-expressing neurons in awake marmosets exhibited rapid changes in activity during photostimulation experiments. Similar to previous studies of rhesus monkeys (Diester et al. 2011; Han et al. 2009), we observed both excitatory and inhibitory changes in activity during delivery of light stimuli. Although ChR2 induces excitatory changes in directly stimulated neurons, the pattern of excitation and inhibition that occurs in cortex likely reflects changes in neural activity that occurred across the network of neurons modulated by light stimuli. The preparation developed in the present work comprised a chronically implanted fiber-optic cable and a technique for performing repeated electrode penetrations and single-neuron recordings from the same population over weeks and months. A primary benefit of this approach is to minimize damage from successive fiber penetrations. Previous studies in rhesus monkeys that have implanted fibers into cortex daily have found that due to their size, the fibers cause considerable damage over successive penetration (Geritis et al. 2012). Other studies have developed preparations with optical stimulation delivered outside the cortex through a clear silicone dura, which reduces damage but also introduces complications due to gradual granulation tissue growth beneath the dura (Nassi et al. 2015; Ruiz et al. 2013). The chronic fiber implant in the current study was designed to facilitate long-term recordings in awake animals in which neural substrates are manipulated either during behavioral tasks or to identify functional connectivity. Our ability to record well-isolated neurons and induce changes in neural activity by delivering light stimuli over the course of at least 9 mo suggests that this preparation is stable and particularly suitable for studies with behaving animals.

Marmoset brains are well suited for techniques that use viral techniques to map neural circuits in primates (Watakabe et al. 2015). Notably, AAV transduction in marmosets was not limited to the proximity of the injection site but also was transported in the long-range projections of pyramidal neurons (Fig. 6). We observed preliminary evidence for both anterograde and retrograde labeling with these AAV constructs. Although AAV is often thought to identify primarily antero-

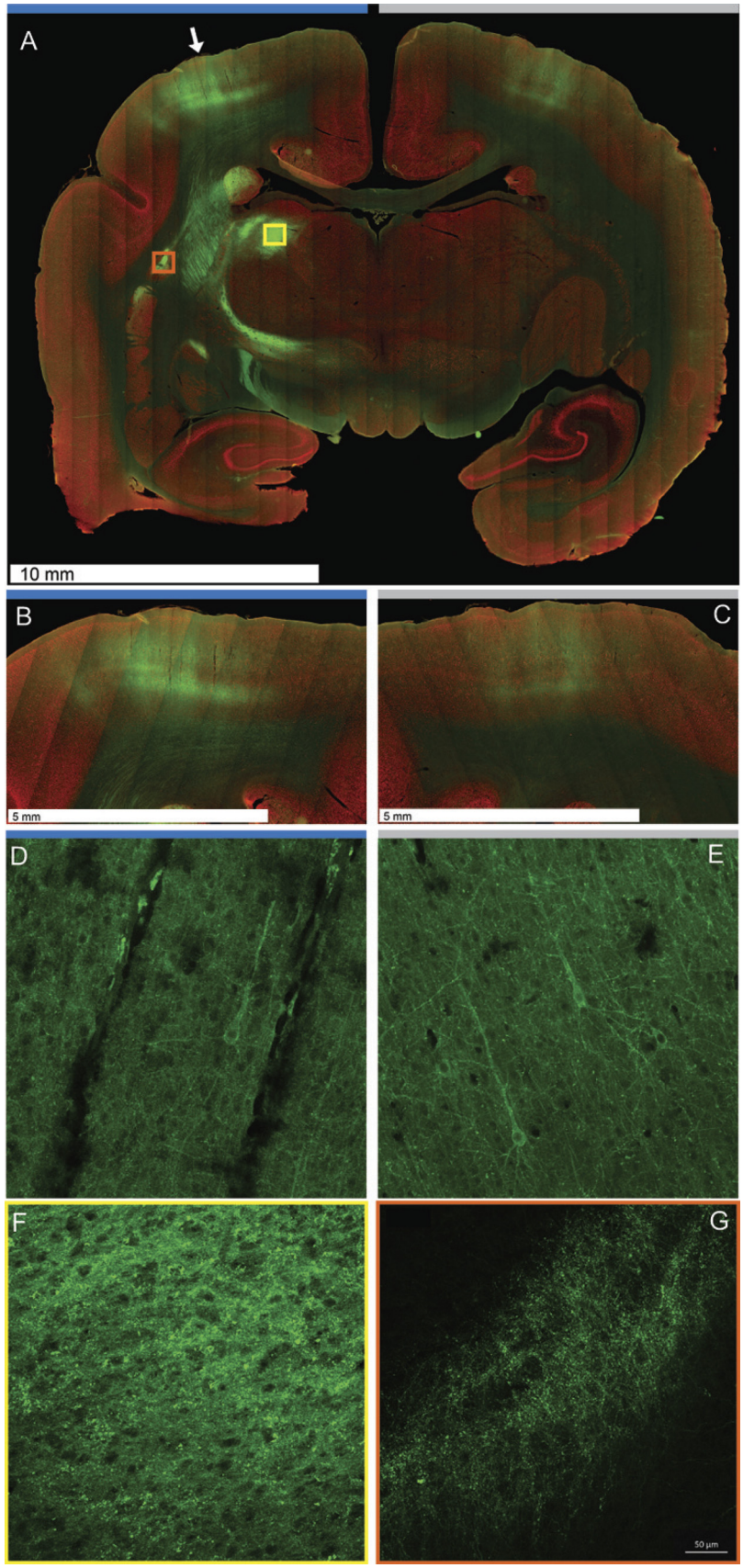

Fig. 6. Neuronal circuit labeling in marmosets with AAV constructs. *A*: micrograph of a whole slice of marmoset brain showing viral expression following an injection of AAV9.hSyn.ChR2.eYFP at both the injection site (white arrow) and contralateral cortex. Transduction is evident in white matter fiber bundles throughout subcortical areas and across corpus callosum. The ipsilateral hemisphere in which the injection was placed is indicated by a blue horizontal bar, whereas the contralateral hemisphere is indicated with a light gray horizontal bar. High magnification shows laminar cortical expression and white matter projections expressing channelrhodopsin-eYFP at the site of injection (*B*) and the contralateral hemisphere (*C*). The ×20 confocal images show eYFP expression in the cell processes and cell bodies at both the ipsilateral (*D*) and contralateral hemispheres (*E*). Subcortical structures generally showed transduction in the cell processes, as evidenced in ventrolateral thalamic motor nucleus (*F*; yellow box in *A*) and putamen (*G*; orange box in *A*). All images shown are from the same tissue section.

grade connections, several other studies of primates have reported retrograde labeling, as well (Masamizu et al. 2011; Salegio et al. 2014; San Sebastian et al. 2013). Similar to work in mice (Oh et al. 2014; Sato et al. 2014), the use of AAV constructs to transduce neurons with opsins and fluorescent proteins may be ideal for identifying pathways in the marmoset brain. The brains of marmosets are small relative to other primates, which may make protein trafficking more tractable than in larger primate models. These initial findings in marmosets may have broad implication, because they suggest that delivering opsins or DREADDS (designer receptors exclusively activated by designer drugs) with viral constructs could be used not only to identify these circuits but also to modulate their activity to test for causal relationships in behavior and disease (Tye and Deisseroth 2012).

The development of optogenetics has led to a veritable renaissance in studies of mammalian neural circuitry (Boyden et al. 2005; Deisseroth 2011). Methods to identify and manipulate populations of neurons with high spatial and temporal precision have yielded insight into the functional properties of the central nervous system underlying complex behavior that was not previously possible (Gunaydin et al. 2014; Guo et al. 2015; Znameskiy and Zador 2013). Although these techniques have been extensively implemented in studies of rodent systems, they have similar potential for elucidating many of the detailed nuances of the primate brain (Afraz et al. 2015; Cavanaugh et al. 2012; Geritis et al. 2012; Jazayeri et al. 2012; Nassi et al. 2015; Ohayon et al. 2013). Data presented in this study suggest that marmosets may be particularly valuable as a model system for application of optogenetic techniques in studies of primate brain function. These methods can be combined with existing behavioral (Chow et al. 2015; Miller and Thomas 2012; Mitchell et al. 2014; 2015; Osmanski et al. 2013; Remington et al. 2012), neurophysiological (Bendor and Wang 2005; Eliades and Wang 2008; Miller et al. 2015; Wang et al. 2005), and neuroimaging approaches (Hung et al. 2015; Liu et al. 2013; Silva et al. 2011) in marmosets to more precisely test the functional architecture underlying primate behavior.

ACKNOWLEDGMENTS

We thank Jennifer Coppola for assistance with the confocal imaging and Chris Petkov for comments on this manuscript.

GRANTS

This work was supported by National Institutes of Health Grants R01DC012087 (to C. T. Miller) and R21MH104756 (to J. F. Mitchell and C. T. Miller) and a Kavli Innovative Research Grant (to J. F. Mitchell and C. T. Miller).

DISCLOSURES

No conflicts of interest, financial or otherwise, are declared by the authors.

AUTHOR CONTRIBUTIONS

M.M., S.U.N., J.F.M., and C.T.M. conception and design of research; M.M., S.U.N., S.C., J.F.M., and C.T.M. performed experiments; M.M., S.U.N., A.D., J.F.M., and C.T.M. analyzed data; M.M., S.U.N., A.D., J.F.M., and C.T.M. interpreted results of experiments; M.M., S.U.N., A.D., J.F.M., and C.T.M. prepared figures; M.M., S.U.N., and C.T.M. drafted manuscript; M.M., S.U.N., A.D., J.F.M., and C.T.M. edited and revised manuscript; M.M., S.U.N., S.C., A.D., J.F.M., and C.T.M. approved final version of manuscript.

REFERENCES

Afraz A, Boyden ES, DiCarlo JJ. Optogenetic and pharmacological suppression of spatial clusters of face neurons reveal their causal role in face gender discrimination. *Proc Natl Acad Sci USA* 112: 6730–6735, 2015.

Belmonte J, Callaway EM, Caddick SJ, Churchland P, Feng G, Homatics GE, Lee K, Leopold DA, Miller CT, Mitchell JF, Mitalipov S, Moutri AR, Movschon JA, Okano H, Reynolds J, Ringach D, Sejnowski TJ, Silva AC, Strick PL, Wu J, Zhang F. Brains, genes and primates. *Neuron* 86: 617–631, 2015.

Bendor DA, Wang X. The neuronal representation of pitch in primate auditory cortex. *Nature* 436: 1161–1165, 2005.

Boyden ES, Zhang F, Bamberg E, Nagel G, Deisseroth K. Millisecond-timescale, genetically targeted optical control of neural activity. *Nat Neurosci* 8: 1263–1268, 2005.

Cavanaugh J, Monosov IE, McAlonan K, Berman R, Smith MK, Cao V, Wang KH, Boyden ES, Wurtz RH. Optogenetic inactivation modifies monkey visuomotor behavior. *Neuron* 76: 901–907, 2012.

Chaplin T, Yu H, Soares J, Gattass R, Rosa MG. A conserved pattern of differential expansion of cortical area as in simian primates. *J Neurosci* 18: 15120–15125, 2013.

Chow C, Mitchell J, Miller CT. Vocal turn-taking in a nonhuman primate is learned during ontogeny. *Proc Biol Sci* 282: 210150069, 2015.

Deisseroth K. Optogenetics. *Nat Methods* 8: 26–29, 2011.

Diester I, Kaufman MT, Mogri M, Pashaie R, Goo W, Yizhai O, Ramakrishnan C, Deisseroth K, Shenoy K. An optogenetic toolbox designed for primates. *Nat Neurosci* 14: 387–397, 2011.

Eliades SJ, Wang X. Neural substrates of vocalization feedback monitoring in primate auditory cortex. *Nature* 453: 1102–1106, 2008.

Geritis A, Farivar R, Rosen BR, Wald LL, Boyden ES, Vanduffel W. Optogenetically induced behavioral and functional network changes in primates. *Curr Biol* 22: 1722–1726, 2012.

Geritis A, Vanduffel W. Optogenetics in primates: a shining future? *Trends Genet* 29: 403–411, 2013.

Goodchild AK, Martin PR. The distribution of calcium-binding proteins in the lateral geniculate nucleus and visual cortex of a New World monkey, the marmoset, *Callithrix jacchus*. *Vis Neurosci* 15: 625–642, 1998.

Gunaydin LA, Gosenick L, Finkelstein JC, Kauvar IV, Fenno LE, Adhikari A, Lammel S, Mirzabekov JJ, Airan RD, Zalocusky KA, Tye KM, Anikeeva P, Malenka RC, Deisseroth K. Natural neural projection dynamics underlying social behavior. *Cell* 157: 1535–1551, 2014.

Guo W, Hight AE, Chen JX, Klapoetke NC, Hancock KE, Shinn-Cunningham BG, Boyden ES, Lee DJ, Polley DB. Hearing the light: neural and perceptual encoding of optogenetic stimulation in the central auditory pathway. *Sci Rep* 5: 10319, 2015.

Han X, Qian X, Bernstein JG, Zhou H, Franzesi GT, Stern P, Bronson R, Graybiel AM, Desimone R, Boyden ES. Millisecond-timescale optical control of neural dynamics in the nonhuman primate brain. *Neuron* 62: 191–198, 2009.

Hung C, Yen CC, Cluchta JL, Papoti D, Bock NA, Leopold DA, Silva AC. Functional mapping of face-selective regions in the extrastriate visual cortex of the monkey. *J Neurosci* 35: 1160–1172, 2015.

Jazayeri M, Lindbloom-Brown Z, Horowitz GD. Saccadic eye movements evoked by optogenetic activation of primate V1. *Nat Neurosci* 15: 1368–1370, 2012.

Kaas JH. Evolution of the neocortex. *Curr Biol* 16: R910–R914, 2006.

Liu JV, Hirano Y, Nascimento GC, Stefanovic B, Leopold DA, Silva AC. fMRI in the awake marmoset: Somatosensory-evoked responses, functional connectivity and comparison with propofol anesthesia. *Neuroimage* 78: 186–195, 2013.

Masamizu Y, Okada T, Ishibashi H, Takeda S, Yuasa S, Nakahara K. Efficient gene transfer into neurons in monkey brain by adeno-associated virus 8. *Neuroreport* 21: 249–258, 2010.

Masamizu Y, Okada T, Kawasaki K, Ishibashi H, Yuasa S, Takeda S, Hasegawa I, Nakahara K. Local and retrograde gene transfer into primate neuronal pathways via adeno-associated virus serotype 8 and 9. *Neuroscience* 193: 249–258, 2011.

Miller CT, Freiwald W, Leopold DA, Mitchell JF, Silva AC, Wang X. Marmosets: a neuroscientific model of human social behavior. *Neuron* 90: 219–233, 2016.

Miller CT, Thomas AW. Individual recognition during bouts of antiphonal calling in common marmosets. *J Comp Physiol A* 198: 337–346, 2012.

Miller CT, Thomas AW, Nummela S, de la Mothe LA. Responses of primate frontal cortex neurons during natural vocal communication. *J Neurophysiol* 114: 1158–1171, 2015.

Mitchell J, Priebe N, Miller CT. Motion dependence of smooth eye movements in the marmoset. *J Neurophysiol* 113: 3954–3960, 2015.

Mitchell J, Reynolds J, Miller CT. Active vision in marmosets: a model for visual neuroscience. *J Neurosci* 34: 1183–1194, 2014.

Mitchell JF, Leopold DA. The marmoset monkey as a model for visual neuroscience. *Neurosci Res* 93: 20–46, 2015.

Nassi JJ, Avery MI, Cetin AH, Roe AW, Reynolds JH. Optogenetic activation of normalization in alert macaque visual cortex. *Neuron* 86: 1504–1517, 2015.

Oh SW, Harris JA, Ng L, Winslow B, Cain N, Mihalas S, Wang Q, Lau C, Kuan L, Henry AM, Mortrud MT, Ouelle B, Nyguyen TN, Sorensen SA, Slaughterbeck CR, Wakeman W, Li Y, Feng D, Ho A, Nicholas E, Hirokawa KE, Bohn P, Joines KM, Peng H, Hawrylcz MJ, Philips JW, Hohmann JG, Wohnoutka P, Gerfen CR, Koch C, Benrnard A, Dang C, Jones AR, Zeng H. A mesoscale connectome of the mouse brain. *Nature* 508: 207–214, 2014.

Ohayon S, Grimaldi P, Schweers N, Tsao DY. Saccade modulation evoked by optical and electrical stimulation in the macaque frontal eye field. *J Neurosci* 33: 16684–16697, 2013.

Osmanski MS, Song X, Wang X. The role of harmonic resolvability in pitch perception in a vocal non-human primate, the common marmoset (*Callithrix jacchus*). *J Neurosci* 33: 9161–9168, 2013.

Remington E, Osmanski M, Wang X. An operant conditioning method for studying auditory behaviors in marmoset monkeys. *PLoS One* 7: e47895, 2012.

Ruiz O, Lusting BR, Nassi JJ, Cetin A, Reynolds J, Albright TD, Callway EM, Stoner GR, Roe AW. Optogenetics through windows in the brain in the nonhuman primate. *J Neurophysiol* 110: 1455–1467, 2013.

Salegio EA, Steeter H, Dube N, Hadaczek P, Samaranch L, Kells AP, San Sebastian W, Zhai Y, Bringas J, Xu T, Forsayeth J, Bankiewicz KS. Distribution of nanoparticles through the cerebral cortex of rodents and nonhuman primates: implications for gene and drug therapy. *Front Neuroanat* 8: 1–8, 2014.

San Sebastian W, Samaranch L, Heller G, Kells AP, Bringas J, Pivirotto P, Forsayeth J, Bankiewicz KS. Adeno-associated virus type 6 is retrogradely transported in the non-human primate brain. *Gene Ther* 20: 1178–1183, 2013.

Sasaki E, Suemizu H, Shimada A, Hanazawa K, Oiwa R, Kamioka M, Tomioka I, Sotomaru Y, Hirakawa R, Eto R, Siozawa S, Maeda T, Ito M, Ito R, Kito C, Yagihashi C, Kawai K, Miyoshi H, Tanioka Y, Tamaoki N, Habu S, Okano H, Nomura T. Generation of transgenic non-human primates with germline transmission. *Nature* 459: 523–527, 2009.

Sato TK, Hausser M, Carandini M. Distal connectivity causes summation and division across mouse visual cortex. *Nat Neurosci* 17: 30–32, 2014.

Seyfarth RM, Cheney DL. Evolution of language from social cognition. *Curr Opin Neurobiol* 28: 5–9, 2014.

Silva AC, Liu JV, Hirano Y, Leoni RF, Merkle H, Mackel JG, Zhang XF, Nascimento GC, Stefanovic B. Longitudinal functional magnetic resonance imaging in animal models. *Methods Mol Biol* 711: 281–302, 2011.

Song X, Osmanski MS, Guo Y, Wang X. Complex pitch perception mechanisms are shared by humans and a New World monkey. *Proc Natl Acad Sci USA* 113: 781–786, 2016.

Spatz WB, Illing RB, Vogt Weisenhorn DM. Distribution of cytochrome oxidase and parvalbumin in the primary visual cortex of the adult and neonate monkey, *Callithrix jacchus*. *J Comp Neurol* 339: 519–534, 1994.

Tye KM, Deisseroth K. Optogenetic investigation of neural circuits underlying brain disease in animal models. *Nat Rev Neurosci* 13: 251–266, 2012.

Wang X, Lu T, Snider RK, Liang L. Sustained firing in auditory cortex evoked by preferred stimuli. *Nature* 435: 341–346, 2005.

Watakabe A, Ohtsuka M, Kinoshita M, Takaji M, Takaji M, Isa K, Mizukami H, Ozawa K, Isa T, Yamamori T. Comparative analyses of adeno-associated viral vector serotypes 1, 2, 5, 8 and 9 in marmoset, mouse and macaque cerebral cortex. *Neurosci Res* 93: 144–157, 2015.

Znameskiy P, Zador AM. Corticostriatal neurons in auditory cortex drive decisions during auditory discrimination. *Nature* 497: 482–485, 2013.